Electron Injection Dynamics of $Ru^{II}(dcbpy)_2(SCN)_2$ on Zirconia

C. M. Olsen, M. R. Waterland, and D. F. Kelley*

Department of Chemistry, Kansas State University, Manhattan Kansas 66506-3701

Received: November 12, 2001; In Final Form: April 8, 2002

The electron injection dynamics of Ru^{II}(4,4′-dicarboxy-2,2′-bipyridine)$_2$(SCN)$_2$ (the so-called N3-dye) adsorbed on colloidal ZrO_2 particles in room-temperature solution have been studied using time-resolved absorption polarization spectroscopy. The solvents used are acetonitrile and methanol. Electron injection is evidenced by the transient absorption anisotropy and/or the wavelength-dependent unpolarized absorption intensity. The results indicate that 630 nm excitation results in no N3* to ZrO_2 electron transfer in both acetonitrile and methanol solvents, 515 nm excitation results in electron injection in acetonitrile, and 495 nm excitation results in electron injection in both acetonitrile and methanol. These results may be understood in terms of simple energetic considerations: 630 nm excitation produces N3* with insufficient energy for electron injection while 495 nm excitation produces N3* with an energy just sufficient for electron injection. In all cases where electron injection is energetically favorable, it occurs very rapidly, <200 fs. There is no indication of rapid (<5 ps) electron injection into deep trap states on the ZrO_2 surface; however, the possibility of rapid injection into shallow trap states cannot be excluded. The observed kinetics also indicate that, following photoexcitation of the adsorbed N3, the ZrO_2 surface relaxes on the 5−10 ps time scale.

Introduction

There has recently been great interest in interfacial electron transfer between sensitizer dyes and semiconductor substrates. Much of this interest has been focused on ruthenium based sensitizer dyes and nanoporous TiO_2, because of the application in photovoltaic cells.[1−3] The dye which has received the most attention is the so-called "N3 dye", $Ru^{II}(dcbpy)_2(NCS)_2$, where dcbpy = 4,4′-dicarboxy-2,2′-bipyridine.[4] Numerous studies have measured the electron injection rates from photoexcited N3 into nanoporous TiO_2 and other types of semiconductor surfaces.[3,5−13] These studies have shown that electron injection into TiO_2 is very fast, with most or all of the injection occurring within 100 fs. While many electron transfer rates are strongly dependent on the nature of the surrounding solvent, the above result is solvent independent. Specifically, fast electron injection is observed for both dry TiO_2 surfaces and TiO_2 surfaces immersed in ethanol.[3,7] This is because the dense manifold of conduction band states is strongly coupled to the photoexcited N3 dye and electron transfer is energetically favorable, independent of the local solvent environment. Molecules that are similar to N3, except having less coupling to the surface, exhibit slower electron injection.[14] Electron injection rates from photoexcited N3 into ZnO and SnO_2 surfaces have been measured to be much slower than those into TiO_2 and nonsingle exponential.[3,9,10] This result is explained in terms of the nature of the orbitals which constitute the semiconductor conduction band. In the TiO_2 case, the orbitals comprising the conduction band have considerable titanium d-orbital character. It is suggested that these orbitals couple more strongly to the N3 π*-donor orbitals than do the metal s-orbitals of ZnO or SnO_2. This point has recently been disputed,[5] so the role of the orbital character in determining the extent of coupling is still somewhat unclear.

Electron transfer can also occur from sensitizer dyes to semiconductor surface states. In cases of large band gap semiconductors, the conduction band is energetically inaccessible and electron transfer can occur only to localized surface states. Despite the inaccessibility of the conduction band, electron injection can occur very efficiently.[15] This type of electron transfer reaction may be quite sensitive to the surrounding solvent for several reasons. An electron in a surface state can be stabilized by the local polar solvent environment. As a result, one might expect this type of electron transfer to be more susceptible to solvent effects than an electron transfer directly into the semiconductor conduction band. The nature of the solvent can also affect the semiconductor surface chemistry, and this can affect the dynamics of electron transfer from adsorbates to semiconductor surface states. The solvent can affect the depth and density of surface trap states and thus the energetics of interfacial electron transfer. Furthermore, the nature of the solvent can also affect adsorbate/surface binding, which can alter the donor/acceptor electronic coupling.

In addition to studies of electron transfer from relaxed sensitizers, there has been considerable interest in the possibility of electron injection from vibrationally unrelaxed states of the photoexcited dye.[3,13,16−19] In many cases, electron injection has been shown to occur on a time scale comparable to or faster than vibrational relaxation. Thus, it is a reasonable speculation that a significant (and perhaps dominant) path for electron injection is from the initially excited Franck−Condon state of the dye, rather than from a relaxed state. The electron injection dynamics of several different ruthenium-type dyes having different excited state oxidation potentials have been studied, and ultrafast electron injection has been shown to occur in several different cases.[3] Dyes having oxidation potentials below the TiO_2 conduction band were excited to high levels from which electron injection could occur in competition with vibrational relaxation. The results indicate that relaxation and

* To whom correspondence should be addressed. E-mail: dfkelley@ksu.edu.

10.1021/jp014160o CCC: $22.00
Published on Web 05/25/2002

electron injection occur on comparable time scales and that some (but not all) of the excited state population undergoes electron injection prior to relaxation. Although excitation wavelength dependent studies have not been performed, excitation to the lowest vibrational levels of the dye would have presumably resulted in little or no electron injection. A similar conclusion results from visible/near-IR time-resolved N3/TiO_2 studies.[13]

In this paper we examine the roles of excitation wavelength and the solvent on the dynamics of N3*/ZrO_2 interfacial electron transfer. This is done by observing the relaxation and electron injection dynamics of photoexcited N3 absorbed on colloidal ZrO_2 particles. The N3/ZrO_2 particles are dissolved in either methanol or acetonitrile solvents at room temperature, and the spectra and dynamics are compared to those obtained for N3 in the neat solvent, lacking the ZrO_2 particles. The dynamics are observed to be critically dependent on the excitation wavelength. We also observe somewhat different electron transfer dynamics in the two solvents, despite using the same ZrO_2 particles in both solvents. The solvent dependent absorption spectra of N3 adsorbed on ZrO_2 particles show that the N3/ZrO_2 electronic coupling is very strong in both solvents, although slightly stronger in acetonitrile.

Experimental Section

ZrO_2 particles used in these studies are prepared by the acid hydrolysis of $ZrCl_4$, as previously described.[15] Specifically, 2.5 g of $ZrCl_4$ (Alfa) is dissolved in 40 mL of anhydrous methanol. The solution is cooled to 0 °C, acidified with 0.125 mL of concentrated HCl and 1.0 mL of distilled H_2O, and allowed to warm to room temperature while being stirred for 2 h. This solution is then heated to reflux for 2 h. This procedure has been reported to produce 10−20 nm particles. The solution is then rotoevaporated to dryness. At this point the particles are resuspended in either acetonitrile or anhydrous methanol. The solvent is then evaporated off under vacuum at room temperature. Several cycles of resuspension followed by solvent evaporation are used to remove as much water as possible. The particles are finally resuspended in either acetonitrile or methanol to form ZrO_2 stock solutions having concentrations of approximately 25 mg/mL. This procedure results in a small amount of particle aggregation. The larger particles result in light scattering, which is a problem in the optical measurements. The solutions are therefore filtered through 0.22 μm Millipore filters prior to the addition of dissolved N3. Filtration removes the larger particles, resulting in clear solutions. We note that the acetonitrile and methanol solutions are derived from the same particles. Each has simply been washed in the appropriate solvent to remove water. The solutions are never neutralized, and the particles are thus probably somewhat acidic.

N3/zirconia samples are made by combining equal volumes of N3/acetonitrile or N3/methanol stock solutions (ca. 50 mM) with the appropriate ZrO_2 stock solutions. It is possible to assess the fraction of N3 dyes that attach to the zirconia particles, as opposed to remaining free in solution. This is done from rotational diffusion measurements. Attachment to the relatively large zirconia particles is expected to dramatically slow the N3 rotational diffusion rate. The zirconia particles are expected to rotationally diffuse on a time scale of many nanoseconds,[20] and N3 attached to the particle surface will undergo rotational diffusion on the same time scale. In contrast, N3 in solution rotationally diffuses on the hundreds of picoseconds time scale.[21] The results presented below show no detectable rotational diffusion on the hundreds of picoseconds time scale, indicating that the vast majority of the N3 dyes are attached to the zirconia particle surfaces.

In all cases, solvents were thoroughly dried and purified prior to use and stored under dry nitrogen. Methanol was Spectral grade and distilled over iodine-activated magnesium in a nitrogen atmosphere. Acetonitrile was HPLC grade and distilled over anhydrous P_2O_5 in a nitrogen atmosphere. N3 dye was obtained from Dr. S. Ferrere at NREL and used without further purification. Samples were held in 1 cm path length sealed cells, and rapidly stirred with a magnetic stir bar. In all cases, samples were filtered with 0.22 μm Millipore filters and degassed immediately before being sealed in the optical cells. N3 dye has labile thiocyanate ligands that are easily hydrolyzed, and we have found that the above purifications are necessary to avoid hydrolysis of the dye. Over the course of the experiments there was no detectable change in the sample absorption spectrum, and we conclude that the above procedures result in N3/ZrO_2/acetonitrile samples that are sufficiently dry to prevent N3 hydrolysis. We note, however, that while the above procedure removes water that is not adsorbed onto the particle surface, the particles are never heated under vacuum and therefore retain much of the adsorbed water.

Time-resolved absorption measurements were made using the femtosecond absorption spectrometer described in a previous publication.[21] Briefly, the femtosecond light source is based on a Clark-MXR 2001. This produces 775 nm, 130 fs, 800 μJ pulses at a repetition rate of 1 kHz. About 4% of the pulse intensity is split off, attenuated, and either used for the sample probe or used to generate white light continuum. In the latter case, wavelength selection is accomplished using 10 nm bandpass interference filters. The remainder of the 775 nm beam is used to pump an OPA (Clark-MXR, vis-OPA). The output of the OPA is approximately 10 μJ fs pulses, tunable throughout the visible region of the spectrum. This tunable output is used for sample excitation; specifically, results following 495, 515, and 630 nm excitation are presented here. The pump beam is typically focused to a spot size of 0.5−1.0 mm at the sample. The power density can be varied by changing the position of the sample with respect to the focal point of the pump beam. In the results presented here, variation of the power density by a factor of about 10 has no detectable effect on the observed kinetics.

The low intensity probe beam is split into reference and sample probe components. The intensity of the probe pulses is less than 1 μJ at the sample. After the sample, the probe beam is split into horizontal and vertical polarization components. These beams and the I_0 beam are imaged onto UDT Sensors PIN 13DI photodiodes, biased at −15 V. The photodiode outputs are amplified and input into an SRS gated integrator. The gated integrator output is measured using an Analog Devices 16 bit analog-to-digital (A/D) converter in the data acquisition computer. The A/D converter and gated integrator triggering and reset are synchronized with the CPA 2001 Q-switch and controlled by home-built timing electronics. Data acquisition is controlled by LabView software running on a Pentium II computer.

Results and Discussion

In this section we discuss the use of transient absorption spectroscopy (polarized and unpolarized) to elucidate the dynamics of electron injection. This discussion is based on the known spectroscopic properties of the N3 metal-to-ligand charge transfer (MLCT) excited state and cation and the geometry of the N3 molecule. These spectroscopic and geometric considerations are discussed below. This is followed by the use of these considerations in the analysis of the time-resolved results

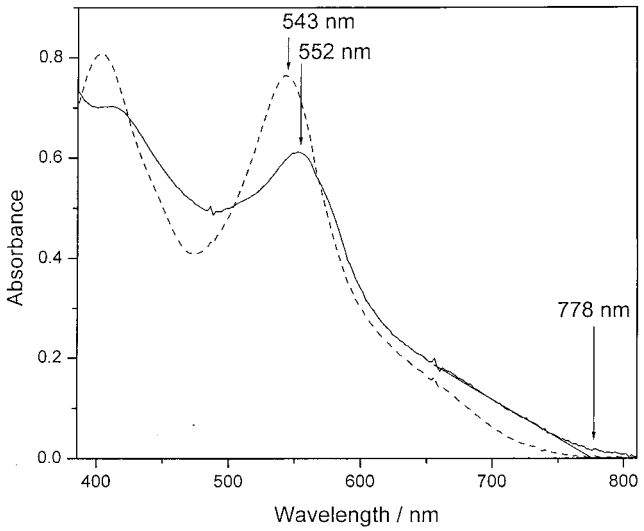

Figure 1. Absorption spectra of N3 in acetonitrile solution (dashed curve) and N3/ZrO_2 in acetonitrile solution (solid curve). The lowest energy absorption maximum of each spectrum is indicated. Also shown is an extrapolation of the red edge of the N3/ZrO_2 absorption to zero absorbance, 778 nm.

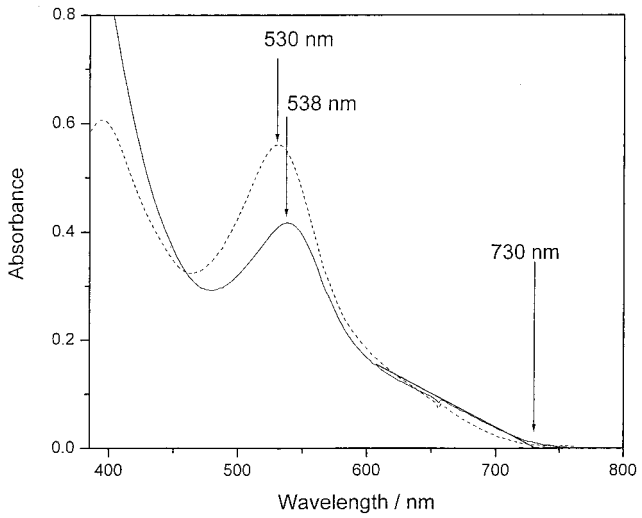

Figure 2. Absorption spectra of N3 in methanol solution (dashed curve) and N3/ZrO_2 in methanol solution (solid curve). The lowest energy absorption maximum of each spectrum is indicated. Also shown is an extrapolation of the red edge of the N3/ZrO_2 absorption to zero absorbance, 730 nm.

on the N3/ZrO_2/solvent systems. The central dynamical question about the N3/zirconia systems is whether electron transfer occurs from the MLCT excited state to the zirconia particles and, if so, what the electron transfer rates are. There are several ways that this question may be addressed. Most commonly, these dynamics are addressed through the use of time-resolved infrared spectroscopy. Alternatively, the electron transfer as well as the intramolecular relaxation dynamics of the adsorbed dye may be addressed by the use of time-resolved absorption polarization spectroscopy. The analysis and interpretation of these results is definitive and straightforward but not immediately obvious. We therefore analyze and discuss the probe wavelength dependent absorption intensity and polarization differences between the N3 MLCT excited state and cation, below. From this analysis and the comparison of the transient spectra obtained in a pure solution (no zirconia) and adsorbed onto solution phase zirconia particles, the electron transfer dynamics are elucidated.

Unpolarized Spectroscopy of N3* and $N3^+$. The absorption spectra of N3 in acetonitrile and methanol solutions as well as adsorbed on ZrO_2 particles in these solvents are shown in Figures 1 and 2. The spectrum of N3 in methanol solution (ca. 4×10^{-5} M) shows a lowest energy MLCT absorption peak at 530 nm. The spectrum of an analogous sample containing ZrO_2 particles (at approximately the same N3 concentration) is also shown. In this case, the MLCT peak shows a slight ($\cong$8 nm) shift to the red. This is due to the perturbation of the MLCT transition by the presence of the zirconia surface. The ZrO_2 particles absorb below 425 nm, and this is also seen in the N3/ZrO_2 spectrum. Qualitatively similar, but somewhat larger differences are observed in the case of acetonitrile solvent. In this case there is an $\cong$9 nm red shift of the lowest energy MLCT peak. This peak also shows considerable broadening when the N3 is attached to the zirconia. Taken together, these spectra indicate that the N3 binds to the zirconia, independent of the nature of the surrounding solvent. They also show a slightly greater spectral perturbation, indicating slightly stronger electronic coupling in the acetonitrile case.

Excitation results in an MLCT excited state in which the ruthenium is in the 3+ state and an electron is localized in a π^* orbital of one of the 4,4′-dicarboxy-2,2′-bipyridine (dcbpy) ligands.[22] Subsequent electron transfer to the zirconia surface removes this π^* electron. Despite the fact that in both cases the ruthenium is in the 3+ state, there are significant spectral differences between the N3 MLCT excited state and the N3 cation. The spectra of both species in ethanol solution have been reported and carefully compared.[6,7,13,17,23] In both cases there is a strong absorption in the red to near-infrared spectral region, which is assigned to a thiocyanate to Ru^{3+} ligand-to-metal charge transfer (LMCT) transition. The presence of the electron in the dcbpy π^* orbital (i.e., the MLCT state) results in a considerable shift in this absorption compared to that obtained for the cation. The transient absorption spectrum of the MLCT excited state exhibits an absorption maximum at 720 nm. The N3 cation exhibits a broader, somewhat weaker absorption that peaks at about 800 nm. The two species have the same absorption intensity (i.e., the same extinction coefficients) at about 780 nm. Thus, whereas the MLCT excited state and cation have comparable absorbances at 780 nm, the MLCT state exhibits a larger absorbance at bluer wavelengths. The N3 ground state also has significant absorbance at wavelengths below 700 nm. Excitation bleaches this transition and thus results in an isosbestic point at about 620 nm upon formation of the MLCT state. Similarly, an isosbestic point is obtained further to the red, at about 650 nm if the cation is formed. The spectral differences between the MLCT excited state and the N3 cation can be used to elucidate electron injection dynamics. Specifically, the N3 MLCT state exhibits a strong absorption in the 620−800 nm spectral region, and electron injection reduces the intensity of this absorption. This is particularly true in the bluest part of this region, 600−700 nm. The above differences between the N3* and $N3^+$ spectra are clearly observed in time-resolved N3/TiO_2 studies examining this spectral range.[13]

Polarization Spectroscopy of N3* and $N3^+$. The polarization spectroscopy of the N3 MLCT excited state and cation may be analyzed in terms of the pseudooctahedral geometry depicted in Figure 3.[21] Excitation results in an MLCT state in which an electron is localized on a single bipyridine ligand, and polarized excitation therefore photoselects one of the bipyridines. The MLCT transition is therefore polarized along a vector from the ruthenium, bisecting one of the bipyridines. The coordinate axes in Figure 3 are chosen such that the photoselected bipyridine is between the $-x$- and $+z$-axes. The red and near-IR transient

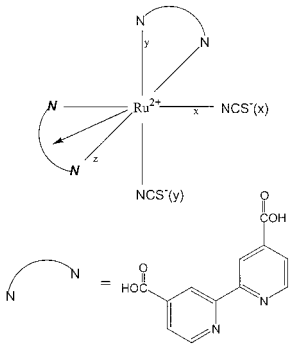

Figure 3. Geometry of the N3 molecule. The axes are chosen such that the photoselected bipyridine ligand (indicated with bold italics) is on the $-x$- and z-axes. The *syn*- and *anti*-thiocyanate ligands are on the y- and x-axes, respectively.

absorption is due to thiocyanate to ruthenium LMCT transitions that are polarized along the thiocyanate to ruthenium axes, the x- and y-axes. Thus, the angle (denoted as θ) between the MLCT excitation vector and the LMCT vector associated with the *syn*-thiocyanate (on the y-axis) is 90°. Similarly, the angle between the MLCT excitation vector and the LMCT vector associated with the *anti*-thiocyanate (on the x-axis) is 135°. Photoselection theory allows calculation of the time-dependent anisotropy in terms of the angle between pump and probe transition vectors, θ. Specifically[24,25]

$$r(t) = (A_{par} - A_{perp})/(A_{par} + 2A_{perp}) = (2/5)P_2(\cos\theta)\exp(-t/\tau_{rot}) \quad (1)$$

where A_{par} and A_{perp} are the absorption intensities having polarizations parallel and perpendicular to that of the pump pulse, $P_2(\cos\theta)$ is the second Legendre polynomial

$$P_2(\cos\theta) = (1/2)(3\cos^2\theta - 1)$$

θ is the angle between the pump and probe transitions and τ_{rot} is the rotational diffusion time. The denominator in eq 1, $A_{par} + 2A_{perp}$, is the total, unpolarized absorption and is independent of interligand electron transfer or rotational diffusion. The initial ($t = 0$) anisotropies of the LMCT transitions associated with the *syn*- and *anti*-thiocyanate ligands are therefore -0.20 and $+0.10$, respectively. The observed anisotropy will be between these extremes, and will depend on the relative intensities of these LMCT transitions. If the absorption intensities of the two LMCT transitions are the same, then a net anisotropy of -0.05 is obtained. This is the case in the N3 cation, in which the thiocyanate ligands are equivalent. Since the two thiocyanate ligands are not equivalent in the N3 MLCT state, the spectra of the two LMCT transitions are not expected to be identical and the observed anisotropy will be probe wavelength dependent in this case. The rotational diffusion time depends on the hydrodynamic radius of the chromophore. In the case of N3 in simple solvents, this is on the order of 100 ps.[21] The ZrO_2 particles to which the N3 dyes are attached are comparatively large (10−20 nm), and since the rotational diffusion time is proportional to the particle volume,[20] the ZrO_2 particles and attached dyes rotationally diffuse on a much longer time scale.

A simple conclusion follows from the above considerations: prior to rotational diffusion, red and near-IR LMCT absorption of the N3 cation will exhibit a negative anisotropy. In the ideal case (no interfering transitions, no mixing with other states, no saturation of the transition), this anisotropy is -0.05. This negative anisotropy is expected to be probe wavelength independent. The presence of an electron in one of the bipyridine π^* orbitals (the N3 MLCT excited state) perturbs the LMCT transitions, complicating the above analysis. The presence of the π^* electron shifts the LMCT transition about 80 nm to the blue. This spectrum is the superposition of the two separate (syn and anti) LMCT spectra. Simple electrostatic considerations suggest that the transition associated with the *anti*-thiocyanate should be shifted less than that associated with the syn ligand. (The reaction field from the solvent stabilizes the *anti*-LMCT dipole, but is orthogonal to the *syn*-LMCT dipole.) Thus, in the absence of interligand electron transfer or rotational diffusion, the absorption anisotropy is expected to be positive of -0.05 when probed to the red of 720 nm (the LMCT absorption maximum) and approaching $+0.10$ at the furthest red wavelengths, at which only the *anti*-LMCT transition is probed. Previous studies on N3 in solution have shown that the initial 775 nm probe anisotropy is about $+0.04$, in agreement with this expectation.[21] Interligand electron transfer interchanges the roles of *syn*- and *anti*-LMCT transitions, and following interligand electron transfer, both are probed equally. Thus, following interligand electron transfer (but prior to rotational diffusion), an anisotropy of -0.05 is expected. An important conclusion may be drawn from the above considerations: A positive anisotropy at 775 nm indicates the presence of the N3 MLCT excited state. This anisotropy may become negative as a result of either cation formation or interligand electron transfer. Since both interligand electron transfer and cation formation result in negative anisotropy, no conclusion may be drawn from the observation of a negative anisotropy.

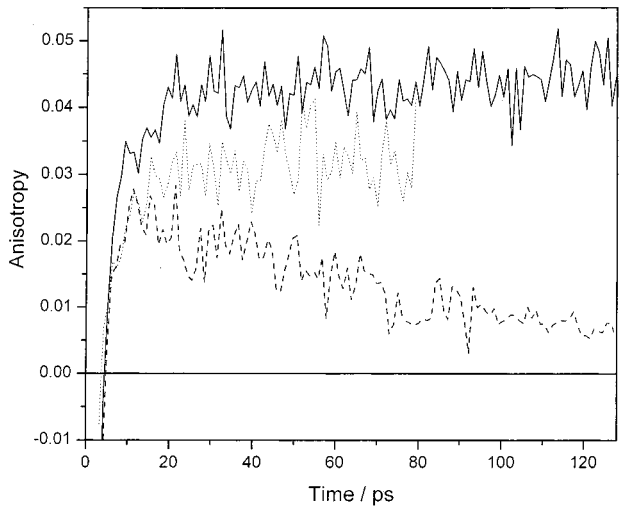

Figure 4. Experimental plots of the 775 nm absorption anisotropy for N3/ZrO_2/acetonitrile (solid line), N3/ZrO_2/methanol (dotted line), and N3/acetonitrile (dashed line), following 630 nm excitation.

Dynamics of N3 on Zirconia Following 630 nm Excitation. Figure 4 shows the photoinduced 775 nm transient absorbance anisotropy obtained following 630 nm excitation of N3 in acetonitrile and adsorbed onto zirconia particles in acetonitrile. A similar result, obtained in N3 on zirconia particles in methanol, is also shown in Figure 4. The N3/methanol (not shown) and N3/acetonitrile results are virtually identical to those reported in a previous paper.[21] The N3/methanol and N3/acetonitrile results show an initially positive anisotropy that subsequently decays as interligand electron transfer and rotational diffusion occur. The anisotropy kinetics obtained for N3/ZrO_2/acetonitrile and N3/ZrO_2/methanol show similar positive anisotropies and no subsequent decay on the 100 ps time scale. As mentioned above, the lack of any detectable anisotropy decay due to rotational diffusion indicates that the vast majority of

the N3 dyes are attached to the zirconia particles, rather than in solution. Since either interligand electron transfer or electron injection results in a negative anisotropy, this result shows that these processes do not occur on the 100 ps time scale following 630 nm excitation. The absence of both interligand electron transfer and of electron injection are easy to understand, and are discussed below.

Electron injection does not occur because the ZrO_2 conduction band is energetically inaccessible following 630 nm excitation. This can be seen from the N3 and ZrO_2 electrochemical potentials, and both potentials must be considered. The oxidation potential of the relaxed N3 MLCT state is about -0.8 V (vs SCE).[4] The redox potential of the ZrO_2 conduction band is best determined in comparison to the more heavily studied material, TiO_2. The TiO_2 conduction band potential follows Nernstian behavior, and is given (in volts) by $-0.400 - 0.06$pH, versus SCE.[26] The ZrO_2 conduction band potential is about 1.15 V more negative than that of TiO_2.[27] This difference is approximately pH independent. Thus, in the pH range of 0−2 (appropriate for the acidic conditions under which these particles are synthesized), the ZrO_2 potential is at about -1.55 to -1.65 V versus SCE.[22,28] Although the above seems quite straightforward, the present studies were performed in nonaqueous solvents and several points about the use of these redox potentials need to be mentioned. The conduction band potentials of metal oxide semiconductors are pH dependent and well-defined only in an aqueous environment. Furthermore, the TiO_2 redox potential is known to be strongly dependent on the nature of the nonaqueous solvent.[29] However, the zirconia samples are prepared through the acidic hydrolysis of $ZrCl_4$, and never thoroughly dried. As a result, even in acetonitrile solutions there is probably still a fair amount of water adsorbed on the zirconia surfaces. (The presence of adsorbed water is also indicated by the relaxation dynamics of adsorbed N3, discussed below.) Thus, despite the nonaqueous environment, the above value of the ZrO_2 conduction band potential is a reasonable estimate. Recent studies on the pH dependence of the energetics of N3/TiO_2 electron injection also bear on the energetic considerations here.[30,31] These studies show that, as the potential of the TiO_2 conduction band changes with pH, the redox potential of adsorbed N3 or similar molecules changes almost as much. This is due to the fact that the ionic environment of the N3 changes along with that of the metal oxide surface. The conclusion resulting from the above considerations is that the ZrO_2 band edge is about 0.8 V above the reduction potential of the relaxed N3 MLCT state and that electron injection is that amount energetically unfavorable. This value is probably accurate to about ± 0.1 V.[27]

Photoexcitation of the N3 molecule does not, in general, produce a relaxed MLCT state. The amount of vibrational and solvent polarization energy that excitation puts into the N3 molecule may be estimated from the excitation wavelength and the N3 absorption spectrum. This is easily done if the ground and MLCT excited states are considered offset classical oscillators with a thermal population on the lower curve. The offset coordinate is taken to be the collective solvent polarization coordinate. In this model, the width of the absorption peak is determined by the thermal distribution in the ground state. The N3 ground to excited state reorganization energy[21] is about 1250 cm^{-1}. This reorganization energy and a thermal energy of 208 cm^{-1} results in excitation to the bottom of the MLCT curve having about 5% of the peak absorption intensity. The wavelength corresponding to this excitation may be approximated by a linear extrapolation of the red edge of the absorption spectrum to zero absorbance, i.e., the absorption onset. The onset of the N3 absorption spectrum in acetonitrile is at about 778 nm (see Figure 1). While the red edge of the absorption spectrum is not exactly linear with wavelength, this procedure provides a reasonable estimate of the lowest energy (vibrationally and solvent relaxed) of the MLCT state. Excitation above that wavelength puts energy into the vibrational and solvent polarization degrees of freedom, which may facilitate electron transfer. 630 nm excitation is about 0.37 eV over the absorption onset. Thus, following 630 nm excitation, the N3 molecule has an energy that is about 0.43 eV too low to transfer an electron to the ZrO_2 conduction band. It is also possible that there are energetically accessible trap states associated with the ZrO_2 surface, into which electron transfer could occur. The results presented here indicate that on the time scale of solvent and vibrational relaxation little or no electron transfer into these states occurs. They also indicate that injection into very deep trap states (0.8 V below the conduction band) does not occur from relaxed N3 on the hundreds of picoseconds time scale. This is consistent with spectroelectrochemical results indicating that most of the surface electron trap states are within 0.1−0.2 V of the conduction band edge.[28]

The lack of interligand electron transfer may be understood in terms of breaking of the symmetry between the two dcbpy ligands. Attachment of the N3 to a ZrO_2 surface is presumably qualitatively similar to attachment to a TiO_2 surface, which has been studied. Three carboxylates can bind to the surface, resulting in one of the dcbpy ligands being more strongly bound than the other. Since binding to the surface shifts the absorption to the red, we presume that the π^* orbitals of the more strongly bound ligand are lower in energy. 630 nm is on the red edge of the absorption spectrum, and the MLCT state localized on the lower energy ligand is preferentially excited. The observed spectral shifts are large compared to thermal energies, suggesting that the energy splitting between the two ligands is also large compared to thermal energies, and we conclude that the weakly bound ligand is more than kT higher in energy than the initially populated ligand. Thus, following 630 nm excitation, the π^* electron starts out in the lower energy MLCT state and stays there; both interligand electron transfer and electron injection are energetically uphill.

It is of interest to note the N3/ZrO_2/acetonitrile dynamics that occur in the first 10−20 ps in Figure 4. The figure shows that the anisotropy evolves (specifically, becomes more positive) on the 5 ps time scale. This transient is too slow to be assigned to vibrational relaxation, which typically takes place on a time scale of less than a few picoseconds for large molecules in a polar condensed phase. An assignment of this being due to electron injection may also be ruled out based on the above polarization considerations; electron injection would cause a decrease in the anisotropy. Evidence of dynamics on the 5 ps time scale are also seen in the kinetics of the total unpolarized ($A_{par} + 2A_{perp}$) absorption, Figure 5. The unpolarized absorption of N3/ZrO_2/acetonitrile shows mostly a pulse width limited rise, followed by a smaller amplitude rise on the 5 ps time scale. We note that electron injection would result in a absorption decay, contrary to the observed kinetics. For comparison, the total absorption kinetics of N3/acetonitrile following 625 nm excitation are also shown in Figure 5. The slight decay observed in the N3/acetonitrile kinetics is due to interligand electron transfer dynamics. The N3/acetonitrile kinetics closely correspond to those presented and analyzed in a previous paper.[21] The slow rise is absent in the N3/acetonitrile (no ZrO_2 particles) samples. (The apparent negative absorption at $t = 0$ is present in samples

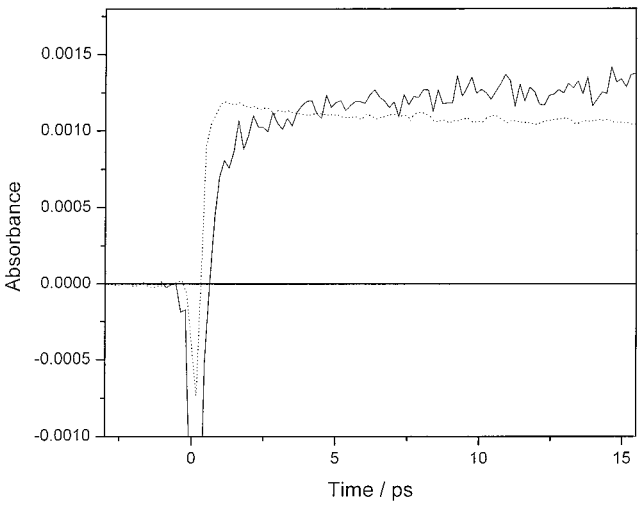

Figure 5. Unpolarized 775 nm absorption kinetics ($A_{par} + 2A_{perp}$) of $N3/ZrO_2$/acetonitrile (solid line) and N3/acetonitrile (dotted line) following 630 nm excitation.

lacking N3 and is due to a four-wave mixing process involving the solvent, and especially the zirconia particles.) We conclude that the absorption spectrum of the N3 MLCT excited state evolves on the 5 ps time scale when the N3 is adsorbed on zirconia particles in an acetonitrile solution. Acetonitrile relaxes on the time scale of a few picoseconds or less,[32] and this is why little evidence of solvent relaxation is apparent in the N3/acetonitrile kinetics shown in Figure 5. Therefore, the observed 5 ps relaxation cannot be associated with surrounding bulk acetonitrile solvent. There are two possible explanations for the presence of this 5 ps transient. First, it may be that acetonitrile relaxes much more slowly in the proximity of the zirconia surface. However, the observed results would require that the relaxation slow by more than an order of magnitude. Solvent dynamics on zirconia surfaces have been measured for the case of H_2O and D_2O, and much smaller effects were reported.[33] Similarly, the reorientation dynamics of CS_2 in confined spaces are observed to slow down compared to the bulk solution, but by less than a factor of 2.[34] Thus, an order of magnitude slowing of the acetonitrile relaxation in the presence of the zirconia surface seems unlikely. Second, it may be that the relaxation is associated with the zirconia surface and that rotational motion of surface hydroxyl groups and/or adsorbed water contribute to this relaxation. Many hydrogen bonding solvents have relaxation components on this time scale,[32,35] and this second possibility seems most likely. Consistent with this explanation, very similar dynamics are seen in the $N3/ZrO_2$/methanol results, also shown in Figure 4. The similarity of these results, along with the absence of this transient without the ZrO_2, suggests that the observed 5−10 ps transient is associated with relaxation of the polar, hydrogen bonding surface environment.

Dynamics of N3 on Zirconia Following 515 and 495 nm Excitation. The results obtained following 515 and 495 nm excitation are considerably different than those obtained following 630 nm excitation. While the 630 nm excitation results show a positive anisotropy, the 515 and 495 nm results show a negative anisotropy. As discussed above, the interpretation of the positive anisotropy is unambiguous: no electron injection or interligand electron transfer occurs. However, a negative anisotropy observed following excitation at 515 or 495 nm could be caused by either electron injection or interligand electron transfer: no conclusive statement can be made. Thus, the dynamics following 515 or 495 nm excitation must be inferred from the magnitudes of the total (unpolarized) absorbance changes and their kinetics.

Figure 6 shows the photoinduced transient absorbance changes at 775, 680, 640, and 600 nm obtained following 515 nm excitation. The figure shows results for N3 in acetonitrile and methanol solvents as well as for N3 adsorbed onto zirconia particles in these solvents. In the results presented in Figure 6, the amplitudes of the transients have been normalized to the amount of the pump intensity absorbed. Since the focal spot sizes, pump energies, and 515 nm sample absorbances are held very close to constant, this normalization corresponds to small corrections.

Figure 6 shows that the 680, 640, and 600 nm transients observed in the N3/methanol, N3/acetonitrile, and $N3/ZrO_2$/methanol samples all exhibit the same transient absorption magnitudes. Very different results are obtained in the case of the $N3/ZrO_2$/acetonitrile sample, with this sample giving smaller absorbances at 680, 640, and 600 nm (negative at 600 nm) than the others. The negative absorbance change at 600 nm indicates that 600 nm is to the blue of the isosbestic point in $N3/ZrO_2$/acetonitrile case and the absorbance change is dominated by the N3 ground state bleach. These results indicate that a different species is formed in the $N3/ZrO_2$/acetonitrile case. Since the excited MLCT state absorbs more strongly than the N3 cation in the 600−700 nm spectral region, these results allow assignment of the transient absorption in the $N3/ZrO_2$/acetonitrile case to the N3 cation. Thus, these comparisons show that electron injection occurs in the $N3/ZrO_2$/acetonitrile case, but not in the $N3/ZrO_2$/methanol case. As a control, the $N3/ZrO_2$/acetonitrile and N3/acetonitrile absorbance changes at 775 nm are also compared. Figure 6 shows that these absorbance transients have approximately the same intensity. Since the MLCT excited state and cation have very nearly the same extinction coefficients at 775 nm, the same absorbance change is expected, independent of whether electron injection occurs. This indicates that the results presented here are consistent with those that show an isosbestic point near 775 nm in the N3* to $N3^+$ reaction.[6,7,13,17,23] It is also important to note that the N3/methanol and N3/acetonitrile samples give essentially identical absorbance changes, indicating that the observed differences in the $N3/ZrO_2$/acetonitrile sample are not simply due to solvent-induced spectral shifts.

The conclusion that $N3/ZrO_2$/acetonitrile undergoes electron injection following 515 nm excitation but does not following 630 nm excitation may be understood in terms of the N3 and ZrO_2 energetics. 515 nm excitation prepares N3 with 0.81 eV of excess (solvent polarization and vibrational) energy. This excess energy permits electron injection into states that would otherwise be energetically inaccessible. This can be thought of as a transient shift of the N3 MLCT state oxidation energy from −0.80 to −1.61 V (vs SCE). Since the ZrO_2 conduction band is at about −1.6 V, this electron transfer process is very close to energetically neutral.

The observed kinetics allow us to put an upper limit on the electron injection time scale. If electron injection in the $N3/ZrO_2$/acetonitrile case occurred on the hundreds of femtoseconds or longer time scale, then the absorbance would initially have an intensity comparable to that observed for N3/acetonitrile, and subsequently decay as electron injection occurs. This behavior is not observed, and we conclude that electron injection takes place on the 200 fs time scale or faster. Furthermore, solvent and vibrational relaxation occur on the 100 fs to 1 ps time scale. Since excitation at lower energies does not result in electron injection, these energy relaxation processes would be

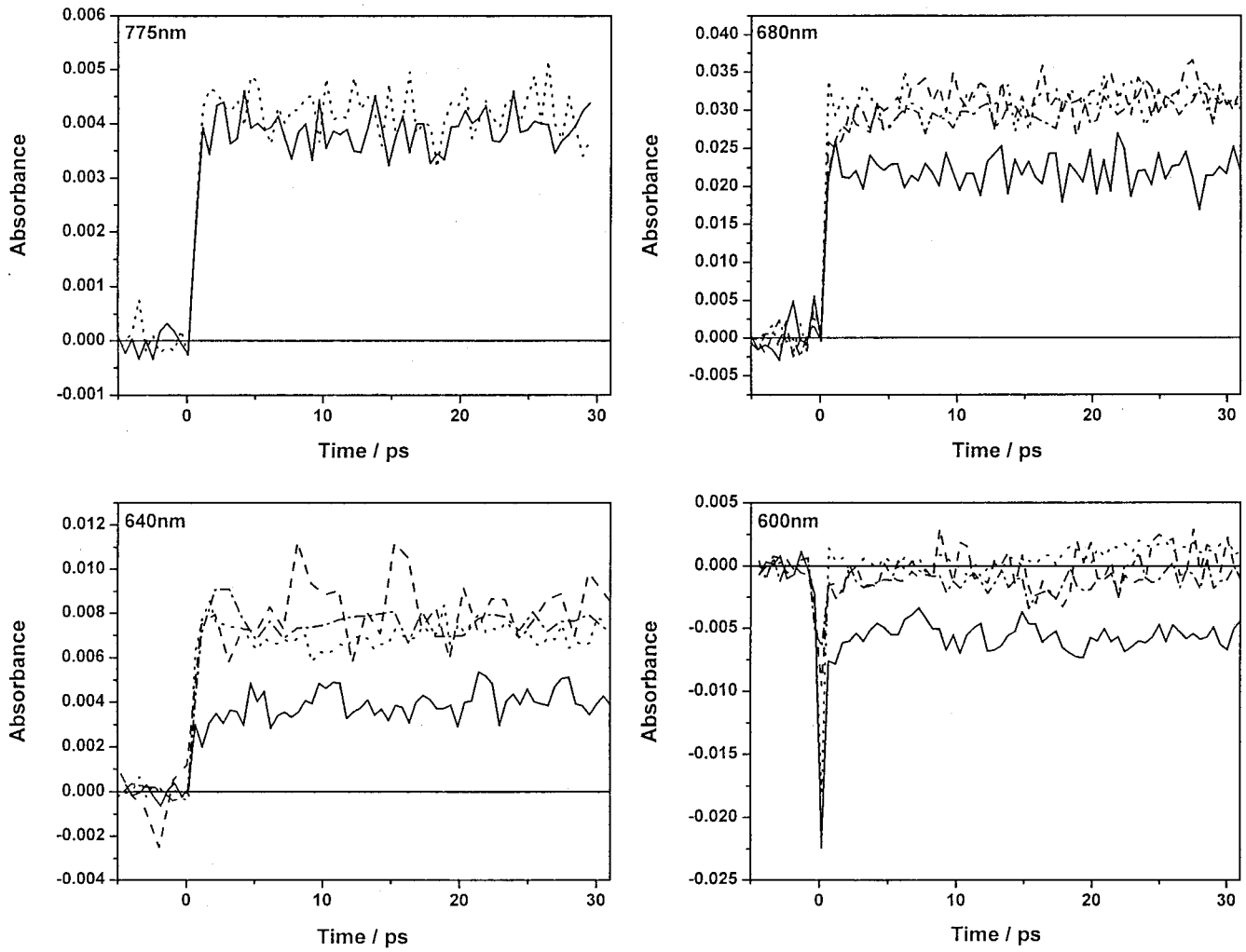

Figure 6. Unpolarized absorption kinetics ($A_{par} + 2A_{perp}$) with probe wavelengths of 775, 680, 640, and 600 nm are displayed. The different samples are indicated as N3/acetonitrile (dotted line), N3/ZrO_2/acetonitrile (solid line), N3/methanol (dot−dash line), and N3/ZrO_2/methanol (dashed line). Excitation is at 515 nm. Note that with probe wavelengths of 600, 640, and 680 nm only the N3/ZrO_2/acetonitrile (solid line) absorbances are smaller, indicating formation of the N3 cation in this case. Also note that the 775 nm probe absorbances for the N3/ZrO_2/acetonitrile and N3/acetonitrile samples are the same, indicating that N3* and $N3^+$ have similar absorbances at this wavelength.

expected to quench the electron injection process. These considerations also indicate that electron injection occurs very rapidly: within the time resolution of this apparatus, in less than 200 fs.

The results obtained for N3/ZrO_2/methanol are more problematic, and perhaps more informative. The results presented in Figure 6 indicate that, following 515 nm excitation, no electron injection occurs in that particular N3/ZrO_2/methanol sample. This result, however, is not consistently reproducible. Some nominally identical N3/ZrO_2/methanol samples indicate that electron injection does occur. Still others show only slight differences between the N3/ZrO_2/methanol and N3/methanol kinetics, indicating that some fraction of the N3 undergoes electron injection. One's initial thought is that in some samples the N3 does not adsorb to the zirconia particles, and is simply in solution. However, the static absorption spectra all show the same shifts in the absorbance maxima, indicating that in all cases N3 is indeed adsorbed onto the particles. These inconsistent results may be understood in terms of the same energetic analysis that was used to understand the N3/ZrO_2/acetonitrile results. In the methanol case, the absorption onset is at about 730 nm and 515 nm excitation results in an N3 molecule with about 0.71 eV of excess energy. This is about 0.1 V less than in the acetonitrile case. This analysis indicates that electron injection for N3/ZrO_2/methanol is very close to energetically neutral, or perhaps slightly energetically unfavorable. It is known that the surface charge of a metal oxide particle can affect its conduction band redox potential. We conclude that very slight differences in sample preparation result in small differences in the ZrO_2 particle potential and hence the inconsistent results following 515 nm excitation. The observation that some samples exhibit partial electron injection indicates that there are significant inhomogeneities within a sample, and perhaps on the surface of each particle. The sample is apparently sufficiently inhomogeneous that there are adsorbed N3 dyes which are, and other absorbed N3 dyes which are not, able to undergo electron injection. This does not appear to occur following 495 nm excitation. Excitation at 495 nm results in the N3 molecule initially having about 0.1 eV more energy than following 515 nm excitation. This is enough that all samples examined undergo electron injection following 495 nm excitation. A comparison of the 640 nm transient absorption kinetics following excitation at 515 and 495 nm is shown in Figure 7. The figure shows that a larger absorbance is obtained for the N3/methanol than for the N3/ZrO_2/methanol sample, indicating electron injection. Comparison of the excitation wavelength dependent N3/ZrO_2/methanol kinetics shows somewhat more absorbance is observed

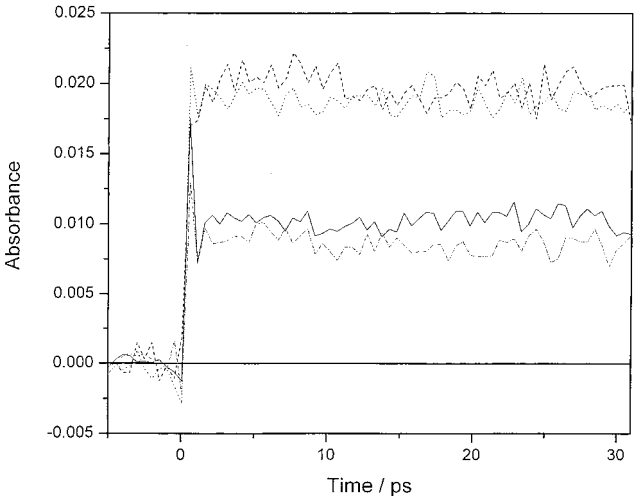

Figure 7. Unpolarized ($A_{par} + 2A_{perp}$) 640 nm absorption kinetics of N3/methanol and N3/ZrO_2/methanol following 495 and 515 nm excitation. The data are indicated as follows: N3/methanol, 515 nm excitation (dashed line); N3/ZrO_2/methanol, 515 nm excitation (solid line); N3/methanol, 495 nm excitation (dotted line); N3/ZrO_2/methanol, 495 nm excitation (dot−dash line). Note that the N3/ZrO_2/methanol 515 nm excitation (solid line) and 495 nm excitation (dot−dash line) curves are lower, indicating formation of the N3 cation in these cases.

following 515 nm, consistent with the assertion that more electron transfer occurs following 495 nm excitation.

It is of interest to note the kinetics that are observed when electron injection is barely energetically favorable, i.e., the 515 nm excitation kinetics in Figure 7. The spike in the absorbance near $t = 0$ may reflect electron injection occurring on the time scale of the instrument response function (about 200 fs). However, there is no evidence of slow (>200 fs) electron injection, which would be indicated by a resolvable absorption decay. It could be argued that this is simply because relaxation very quickly makes electron injection energetically unfavorable. The relaxation dynamics of N3 in methanol have been studied carefully,[21] and bear on this possibility. Relaxation of the N3/methanol absorption following excitation in this wavelength range is due to polarization relaxation of the solvent and occurs on the 5 ps time scale. This is in agreement with the known time scales of methanol polarization relaxation dynamics, which occurs on time scales ranging from subpicoseconds to several picoseconds, with an average relaxation time of about 5 ps.[32] The photoexcited N3 may therefore retain the excess energy and be slightly above the conduction band energy for several picoseconds, facilitating electron injection. All of the above observations indicate that when electron transfer occurs, it does so very rapidly. Electron transfer is energetically favorable only prior to solvent and vibrational relaxation and therefore must compete with these processes to occur efficiently. The large difference between the absorbance changes in the N3/solvent and N3/ZrO_2/solvent samples indicates the electron transfer is quite efficient, and we conclude that it occurs within a few hundred femtoseconds.

To this point we have tacitly assumed that electron injection occurs into the ZrO_2 conduction band. However, metal oxide semiconductors have a high density of surface trap states 0.1−0.2 V below the conduction band.[26,28] If the density of these trap states is sufficiently high, then electron injection into these states may also be occurring in the present case. The electron transfer energetics are known only to within 0.1 or 0.2 V, which is insufficiently accurate to exclude this possibility.

Comparison with Other Electron Injection Processes. The results presented here are consistent with the fast electron injection results observed for N3 on TiO_2 surfaces.[6,8,9,11,36] Similar binding and therefore similar electronic couplings are expected for N3 on TiO_2 and ZrO_2. In the TiO_2 case, the energy of the N3 MLCT state is above the semiconductor conduction band potential, resulting in very fast (<200 fs) electron injection. The results presented here show that the same thing happens when N3 is excited above the ZrO_2 conduction band.

In the present case, photoexcitation at 630 nm results in an N3 excited state which is about 0.5 V below the conduction band. The results presented here indicate that electron transfer to low lying surface states is slow compared to the 5 ps time scale of solvent relaxation. This result is in contrast to those reported for the alizarin/ZrO_2 system, for which fast electron transfer into the ZrO_2 surface states is reported.[15] The difference cannot be due to weak coupling in this case: very fast injection into ZrO_2 conduction band is observed in the present case. Furthermore, the ZrO_2 particles are synthesized in exactly the same manner and would be expected to have similar surface chemistries, and therefore similar densities of trap states. The reason for this discrepancy is unknown.

The above results may also be compared to those obtained for N3 on ZrO_2 nanocrystalline thin films in the presence of ethylene carbonate/propylene carbonate (1:1).[6] No electron transfer was observed following 605 nm excitation, in agreement with results presented here. These studies also indicate that, at most, limited electron injection occurs following 510 nm excitation. Thus, little or no electron injection is observed for N3/ZrO_2 following excitation at either wavelength in the presence of ethylene carbonate/propylene carbonate. This is consistent with the methanol, but not the acetonitrile results presented here. The reason for this difference is not clear. The difference may be due to solvent-dependent shifts in the N3 energetics and that the solvent environment of ethylene carbonate/propylene carbonate does not solvate the adsorbed N3 as well as acetonitrile. These factors may result in electron injection being energetically uphill in ethylene carbonate/propylene carbonate as it is in most methanol samples. Alternatively, the difference may be due to the preparation and history of the ZrO_2 surfaces. We emphasize that 510 or 515 nm excitation produces an N3 excited state that is energetically very close to the ZrO_2 conduction band edge. Very slight energetic differences may put this state slightly above or below the band edge, dramatically changing the electron injection dynamics.

The above observations for both acetonitrile and methanol are consistent with the idea that the electron-donating orbitals on the excited state N3 are strongly coupled to a high density of electronic states at the conduction band edge. If the coupling is sufficiently strong, then the electron transfer is in the adiabatic regime and is essentially barrierless.[37−40] The result can be very rapid electron transfer, <200 fs. This appears to be the case in the N3/ZrO_2/solvent systems.

Conclusions

Several conclusions may be drawn from the results presented here.

1. N3 adsorbs onto colloidal ZrO_2 particles, resulting in a significant perturbation in the absorption spectrum. This indicates strong electronic coupling between N3 and the ZrO_2 particle. This coupling is slightly stronger in the presence of acetonitrile than in methanol.

2. The electron injection reaction from the excited state N3 into colloidal ZrO_2 may be followed using time-resolved polarized absorption spectroscopy of the thiocyanate to ruthenium LMCT band. Both the total absorbance and the absorption

anisotropy can reveal the electron injection dynamics, and the two types of measurements are complementary.

3. The excited MLCT state of N3 undergoes rapid ($\leq$200 fs) electron injection if excited at a sufficiently high energy that the nascent MLCT state is energetically above the ZrO_2 conduction band level. Rapid electron injection into very shallow ($<$0.2 eV) trap states may also occur.

4. If the excitation energy is more than several tenths of an electronvolt below the ZrO_2 conduction band, then rapid electron injection is not observed. If electron injection does occur into deeper trap states, it must be sufficiently slow that it does not compete with solvent and vibrational relaxation.

5. The spectrum of N3 adsorbed on ZrO_2 in acetonitrile solvent evolves on the 5−10 ps time scale following MLCT excitation. Since relaxation in pure acetonitrile occurs on a faster time scale, this indicates that the ZrO_2 surface relaxes on the 5 ps time scale. We speculate that rotational motion of surface hydroxyl groups and/or adsorbed water or methanol contributes to this relaxation.

Acknowledgment. This work was supported by a grant from the U. S. Department of Energy (Grant DE-FG03-00ER15037). M.R.W. also thanks the Foundation for Research, Science and Technology of New Zealand for a New Zealand Science and Technology Postdoctoral Fellowship (Contract No. KSU-901). The authors also thank Dr. S. Ferrere for the sample of N3 dye.

References and Notes

(1) Oregan, B.; Gratzel, M. *Nature* **1991**, *353*, 737.
(2) Hagfeldt, A.; Gratzel, M. *Acc. Chem. Res.* **2000**, *33*, 269.
(3) Asbury, J. B.; Hao, E.; Wang, Y.; Ghosh, H. G.; Lian, T. *J. Phys. Chem. B* **2001**, *105*, 4545.
(4) Nazeeruddin, M. K.; Kay, A.; Rodicio, I.; Humphry-Baker, R.; Muller, E.; Liska, E. P.; Vlachopoulos, N.; Gratzel, M. *J. Am. Chem. Soc.* **1993**, *115*, 6382.
(5) Bauer, C.; Boschloo, G.; Mukhtar, E.; Hagfeldt, A. *J. Phys. Chem. B* **2001**, *105*, 5585.
(6) Tachibana, Y.; Moser, J. E.; Gratzel, M.; Klug, D. R.; Durrant, J. R. *J. Phys. Chem.* **1996**, *100*, 20056.
(7) Moser, J. E.; Noukakis, D.; Bach, U.; Tachibana, Y.; Klug, D. R.; Durrant, J. R.; Humphry-Baker, R.; Gratzel, M. *J. Phys. Chem. B* **1998**, *102*, 3649.
(8) Heimer, T. A.; Heilweil, E. J. *J. Phys. Chem. B* **1997**, *101*, 10990.
(9) Asbury, J. B.; Ellingson, R. J.; Ghosh, N.; Ferrere, S.; Nozik, A. J.; Lian, T. *J. Phys. Chem. B* **1999**, *103*, 3110.
(10) Asbury, J. B.; Wang, Y.; Lian, T. *J. Phys. Chem.* **1999**, *103*, 6644.
(11) Ellingson, R. J.; Asbury, J. B.; Ferrere, S.; Ghosh, H. N.; Sprague, J. R.; Lian, T.; Nozik, A. J. *J. Phys. Chem. B* **1998**, *102*, 6455.
(12) Tachibana, Y.; Haque, S.; Mercer, I. P.; Durrant, J. R.; Klug, D. R. *J. Phys. Chem. B* **2000**, *104*, 1198.
(13) Benkö, G.; Kallioinen, J.; Korppi-Tommola, J. E. I.; Yartsev, A. P.; Sundström, V. *J. Am. Chem. Soc.* **2002**, *124*, 489.
(14) Asbury, J. B.; Hao, E.; Wang, Y.; Lian, T. *J. Phys. Chem. B* **2000**, *104*, 11957.
(15) Huber, R.; Spörlein, S.; Moser, J. E.; Grätzel, M.; Wachtveitl, J. *J. Phys. Chem. B* **2000**, *104*, 8995.
(16) Wang, Y.; Asbury, J. B.; Lian, T. *J. Phys. Chem. A* **2000**, *104*, 4291.
(17) Moser, J. E.; Gratzel, M. *Chimia* **1998**, *52*, 160.
(18) Ferrere, S.; Gregg, B. A. *J. Am. Chem. Soc.* **1998**, *120*, 843.
(19) Lenzmann, F.; Krueger, J.; Burnside, S.; Brooks, K.; Gratzel, M.; Gal, D.; Ruhle, S.; Cahen, D. *J. Phys. Chem. B* **2001**, *105*, 6347.
(20) Fleming, G. R. *Chemical Applications of Ultrafast Spectroscopy*; Oxford: New York, 1986.
(21) Waterland, M. R.; Kelley, D. F. *J. Phys. Chem. A* **2001**, *105*, 4019.
(22) Hagfeldt, A.; Gratzel, M. *Chem. Rev.* **1995**, *95*, 49.
(23) Das, S.; Kamat, P. V. *J. Phys. Chem. B* **1998**, *102*, 8954.
(24) Tao, T. *Biopolymers* **1969**, *8*, 609.
(25) Albrecht, A. *J. Mol. Spectrosc.* **1961**, *6*, 84.
(26) Rothenburger, G.; Fitzmaurice, D.; Gratzel, M. *J. Phys. Chem.* **1992**, *96*, 5983.
(27) Butler, M. A.; Ginley, D. S. *J. Electrochem. Soc.* **1978**, *125*, 228.
(28) Kay, A.; Humphry-Baker, R.; Gratzel, M. *J. Phys. Chem.* **1994**, *98*, 952.
(29) Redmond, G.; Fitzmuarice, D. *J. Phys. Chem.* **1993**, *97*, 1426.
(30) Zaban, A.; Ferrere, S.; Sprauge, J.; Gregg, B. A. *J. Phys. Chem.* **1997**, *101*, 55.
(31) Zaban, A.; Ferrere, S.; Gregg, B. *J. Phys. Chem. B* **1998**, *102*, 452.
(32) Maroncelli, M. *J. Mol. Liq.* **1993**, *57*, 1.
(33) Pant, D.; Levinger, N. E. *J. Phys. Chem. B* **1999**, *103*, 7846.
(34) Loughnane, B. J.; Farrer, R. A.; Scodinu, A.; Reilly, T.; Fourkas, J. T. *J. Phys. Chem. B* **2000**, *104*, 5421.
(35) Horng, M. L.; Gardecki, J. A.; Papazyan, A.; Maroncelli, M. *J. Phys. Chem.* **1995**, *99*, 17311.
(36) Hannappel, T.; Burfeindt, B.; Storck, W.; Willig, F. *J. Phys. Chem. B* **1997**, *101*, 6799.
(37) Gao, Y. Q.; Marcus, R. A. *J. Chem. Phys.* **2000**, *112*, 3358.
(38) Gao, Y. Q.; Marcus, R. A. *J. Chem. Phys.* **2000**, *113*, 6351.
(39) Smith, B. B.; Halley, J. W.; Nozik, A. J. *Chem. Phys.* **1996**, *205*, 47.
(40) Smith, B. B.; Nozik, A. J. *Chem. Phys.* **1996**, *205*, 245.